Electronic Supplementary Material (ESI) for RSC Advances.
This journal is © The Royal Society of Chemistry 2015

Electronic supplementary information

Vanadium(V) tetra-phenolate complexes: Synthesis, structural studies and ethylene homo-(co-)polymerization capability

Carl Redshaw,[a*] Mark J. Walton,[b] Mark R.J. Elsegood,[c] Timothy J. Prior[a] and Kenji Michiue[d]

[a] *Department of Chemistry, University of Hull, Hull, HU6 7RX, U.K.*

[b] *Energy Materials Laboratory, School of Chemistry, University of East Anglia, Norwich, NR4 7TJ, U.K.*

[c] *Chemistry Department, Loughborough University, Loughborough, Leicestershire, LE11 3TU,U.K.*

[d] *Process Technology Center, Mitsui Chemicals Inc., 580-32 Nagaura, Sodegaura, Chiba 299-0265, Japan*

Contents

Crystallography

Figures S1-S7: ORTEP diagrams of the asymmetric units of complexes **1** to **7** with ellipsoids at either 30 or 50 % probability level as stated. Where the structure contains disorder, this is not shown in the interest of clarity.

Figure S8: ORTEP diagrams of spiro compound **I** with ellipsoids at 50 % probability level.

Table S1: Crystal data for spiro compound **I**.

Table S2: Selected bond lengths (Å) and angles (°) for spiro compound **I**.

Figure S9: ORTEP diagrams of spiro compound **II** with ellipsoids at 50 % probability level. Hydrogen atoms are omitted for clarity.

Table S3. Crystal data for spiro compound **II**.

Table S4: Selected bond lengths (Å) and angles (°) for spiro compound **II**.

Figures S10: ORTEP diagrams of the asymmetric unit of complex **8** with ellipsoids at 50 % probability level.

Table S5. ^{51}V NMR spectroscopic data for **1** – **8**.

Catalysis

Ethylene polymerization: results for the effect of co-catalyst and ETA

Table S6. Results for the effect of co-catalyst and ETA on compounds **1 - 3**, **5**, **8** and **[VO(OEt)Cl_2]**.

Figure S11: Ethylene uptake for **1** *versus* time using DMAC (left) and DEAC (right) as co-catalyst.

Figure S12: Ethylene uptake for **1** *versus* time using EADC (left) and Et_3AlCl_2 (SQ) (right) as co-catalyst.

Figure S13: PDI graph for **1** using DMAC, DEAC, EADC and Et_3AlCl_2 (SQ) as co-catalyst.

Figure S14: Ethylene uptake for **2** *versus* time using DMAC (left) and DEAC (right) as co-catalyst.

Figure S15: PDI graph for **2** using DMAC and DEAC as co-catalyst.

Figure S16: Ethylene uptake for **3** *versus* time using DMAC (left) and DEAC (right) as co-catalyst.

Figure S17: Ethylene uptake for **3** *versus* time using EADC (left) and Et_3AlCl_2 (SQ) (right) as co-catalyst.

Figure S18: PDI graph for **3** using DMAC, DEAC, EADC and Et_3AlCl_2 (SQ) as co-catalyst.

Figure S19: Ethylene uptake for **5** *versus* time using DMAC (left) and DEAC (right) as co-catalyst.

Figure S20: PDI graph for **5** using DMAC and DEAC as co-catalyst.

Figure S21: Ethylene uptake for **8** *versus* time using DMAC (left) and DEAC (right) as co-catalyst.

Figure S22: Ethylene uptake for **8** *versus* time using EADC (left) and Et_3AlCl_2 (SQ) (right) as co-catalyst.

Figure S23: PDI graph for **8** using DMAC, DEAC, EADC and Et_3AlCl_2 (SQ) as co-catalyst.

Figure S24: Ethylene uptake for $VO(OEt)Cl_2$ *versus* time using DMAC (left) and DEAC (right) as co-catalyst.

Figure S25: Ethylene uptake for $VO(OEt)Cl_2$ *versus* time using EADC (left) and Et_3AlCl_2 (SQ) (right) as co-catalyst.

Figure S26: PDI graph for $VO(OEt)Cl_2$ using DMAC, DEAC, EADC and Et_3AlCl_2 (SQ) as co-catalyst.

Ethylene polymerization: results for the effect of temperature

Table S7. Effect of temperature on compounds **1 - 3**, **5 - 8** and [$VO(OEt)Cl_2$]

Figure S27: Ethylene uptake for **1** *versus* time using DMAC (left) and DEAC (right) as co-catalyst.

Figure S28: PDI graph for **1** using DMAC and DEAC as co-catalyst.

Figure S29: Ethylene uptake for **2** *versus* time using DMAC (left) and DEAC (right) as co-catalyst.

Figure S30: PDI graph for **2** using DMAC and DEAC as co-catalyst.

Figure S31: Ethylene uptake for **3** *versus* time using DMAC (left) and DEAC (right) as co-catalyst.

Figure S32: PDI graph for **3** using DMAC and DEAC as co-catalyst.

Figure S33: Ethylene uptake for **5** *versus* time using DMAC (left) and DEAC (right) as co-catalyst.

Figure S34: PDI graph for **5** using DMAC and DEAC as co-catalyst.

Figure S35: Ethylene uptake for **6** *versus* time using DMAC (left) and DEAC (right) as co-catalyst.

Figure S36: PDI graph for **6** using DMAC and DEAC as co-catalyst.

Figure S37: Ethylene uptake for **7** *versus* time using DMAC (left) and DEAC (right) as co-catalyst.

Figure S38: PDI graph for **7** using DMAC and DEAC as co-catalyst.

Figure S39: Ethylene uptake for **8** *versus* time using DMAC (left) and DEAC (right) as co-catalyst.

Figure S40: PDI graph for **8** using DMAC and DEAC as co-catalyst.

Figure S41: Ethylene uptake for $VO(OEt)Cl_2$ versus time using DMAC (left) and DEAC (right) as co-catalyst.

Figure S42: PDI graph for $VO(OEt)Cl_2$ using DMAC and DEAC as co-catalyst.

Table S8. Data for runs using **1** and **3** with co-catalysts Me_3Al, Et_3Al and DMAO.

Table S9. Data for runs using **8** and $VO(OEt)Cl_2$ with Me_3Al, Et_3Al and DMAO.

Figure S43. ^{13}C NMR spectrum of polyethylene using complex **2**/Et_3AlCl_2 (run 31, Table S6).

Ethylene/propylene co-polymerization

Figure S44: Ethylene uptake for **1** -**3**, **5** - **8** and $VO(OEt)Cl_2$ *versus* time using DMAC (left) and using DEAC (right) as co-catalyst.

Figure S45: PDI graph for **1** -**3**, **5** - **8** and $VO(OEt)Cl_2$ using DMAC as co-catalyst.

Figure S46: PDI graph for **1** -**3**, **5** - **8** and $VO(OEt)Cl_2$ using DEAC as co-catalyst.

Crystallography

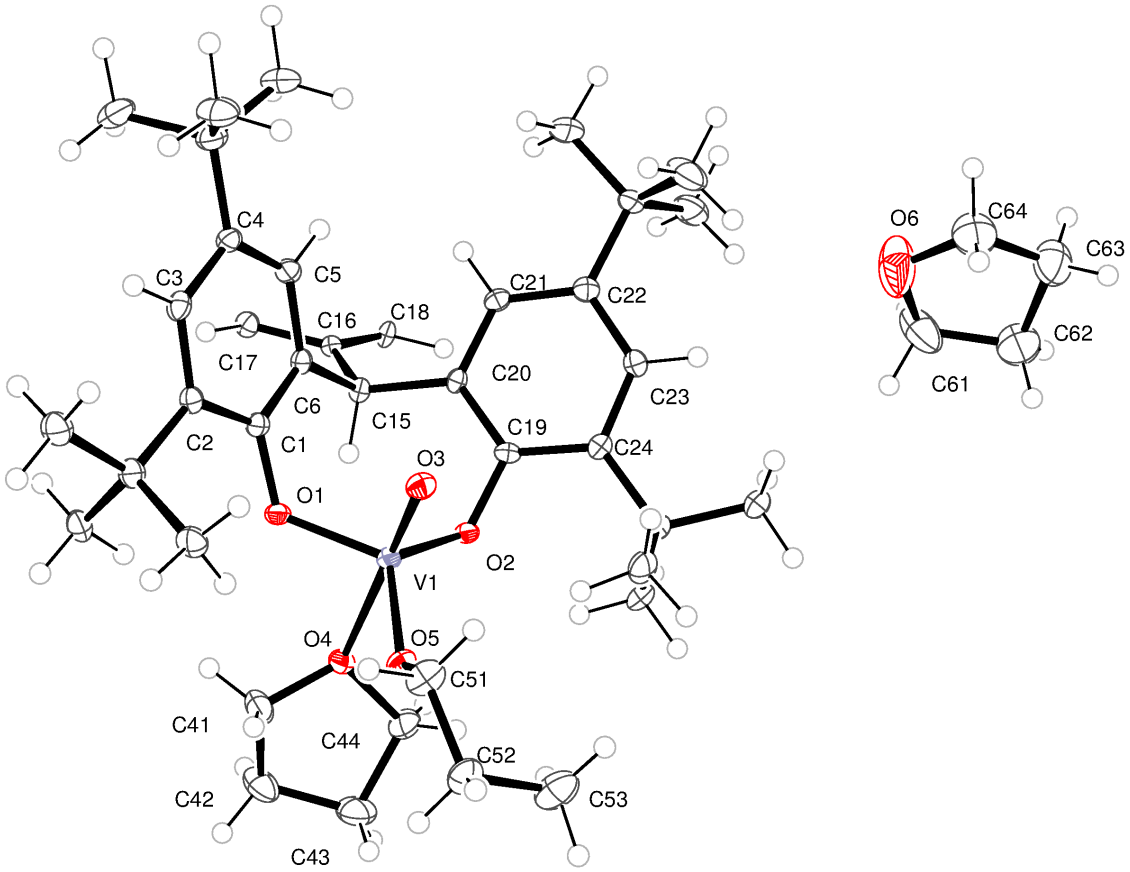

Figure S1. ORTEP diagrams of the asymmetric unit of complex **1** with ellipsoids at 50 % probability level.

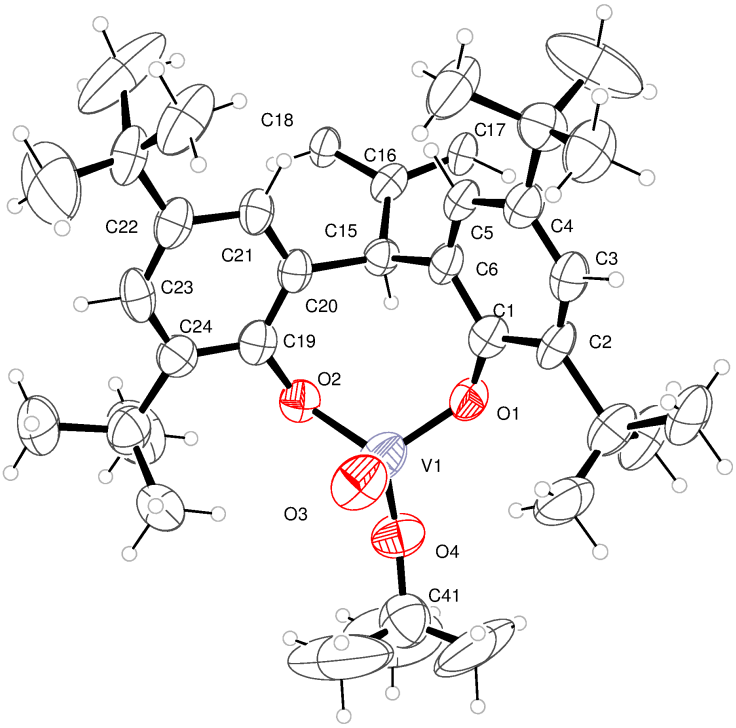

Figure S2. ORTEP diagrams of the asymmetric unit of complex **2** with ellipsoids at 50 % probability level. (Atoms are drawn as 30 % thermal ellipsoids for clarity)

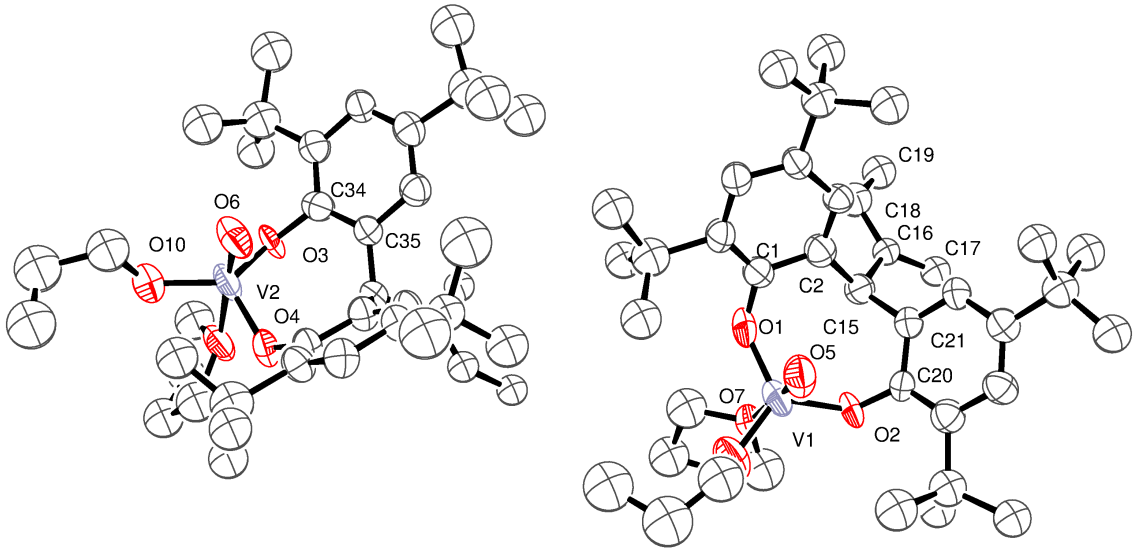

Figure S3. ORTEP diagrams of the asymmetric unit of complex **3** with ellipsoids at 50 % probability level. (Atoms are drawn as 30 % thermal ellipsoids for clarity).

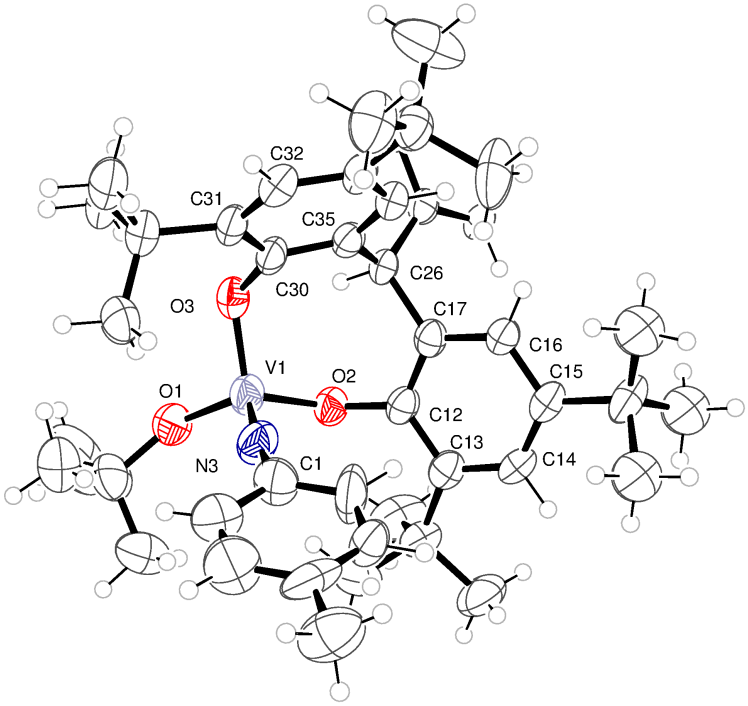

Figure S4. ORTEP diagrams of the asymmetric unit of complex **4** with ellipsoids at 50 % probability le

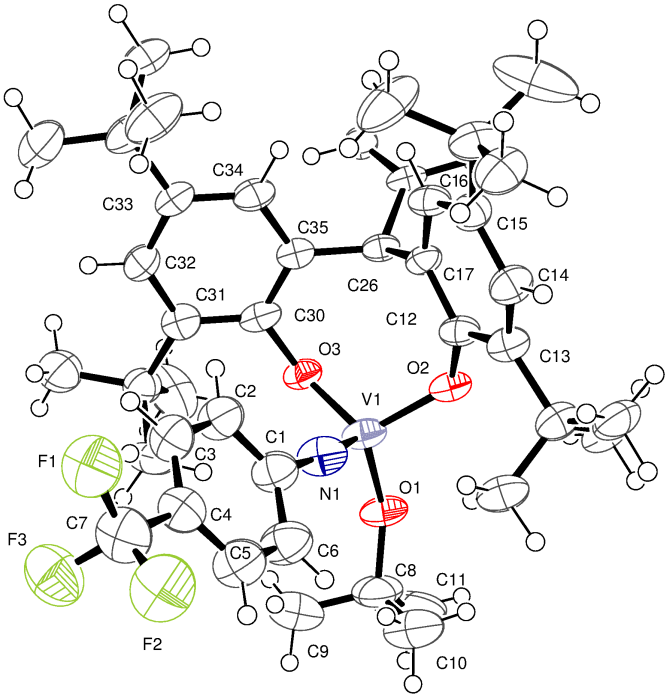

Figure S5. ORTEP diagrams of the asymmetric unit of complex **5** with ellipsoids at 50 % probability level.

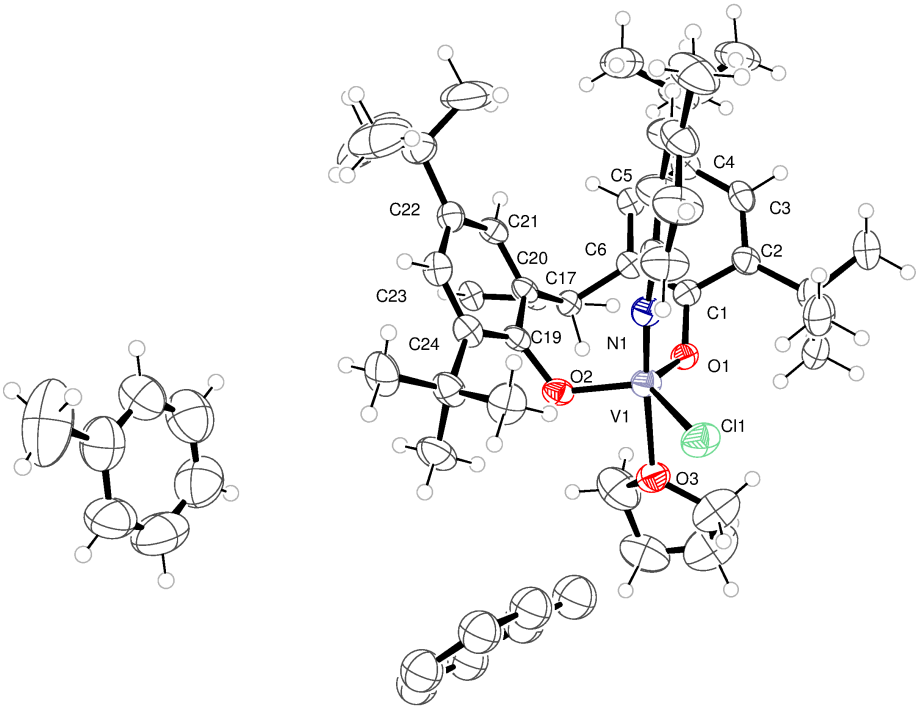

Figure S6. ORTEP diagrams of the asymmetric unit of complex **6** with ellipsoids at 50 % probability level.

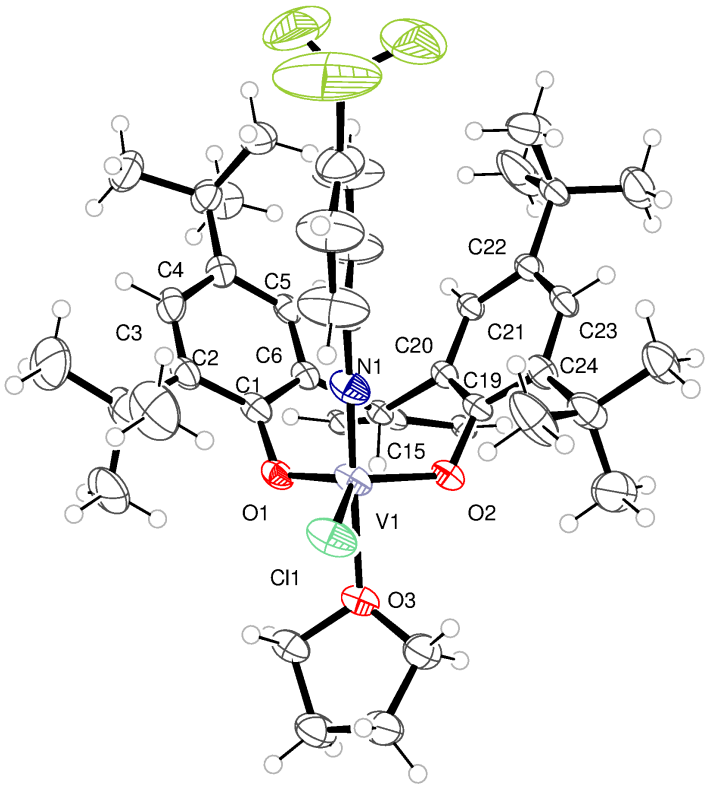

Figure S7. ORTEP diagrams of the asymmetric unit of complex **7** with ellipsoids at 50 % probability level.

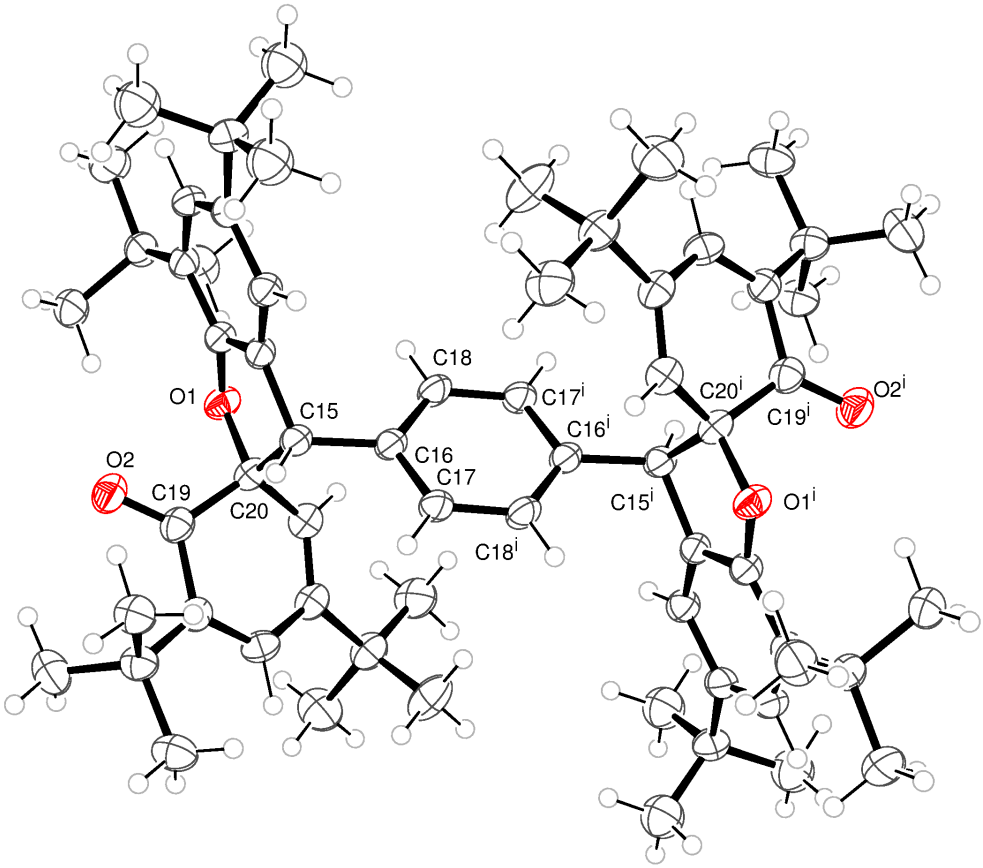

Figure S8. ORTEP diagram of spiro compound **I** with ellipsoids at 50 % probability level.

Table S1. Crystal data for spiro compound **I**.

Empirical formula	$C_{64}\,H_{86}\,O_4$	
Formula weight	919.32	
Temperature	100(2) K	
Wavelength	0.71075 Å	
Crystal system	Monoclinic	
Space group	P 2_1/n	
Unit cell dimensions	a = 10.9672(8) Å	α= 90°.
	b = 18.3003(13) Å	β= 97.721(14)°.
	c = 14.5447(10) Å	γ = 90°.
Volume	2892.7(4) $Å^3$	
Z	2	
Density (calculated)	1.055 Mg/m^3	
Absorption coefficient	0.064 mm^{-1}	

F(000)	1004
Crystal size	0.13 × 0.06 × 0.02 mm^3
Theta range for data collection	2.457 to 27.524°.
Index ranges	-14<=h<=12, -23<=k<=23, -18<=l<=18
Reflections collected	36590
Independent reflections	6556 [R(int) = 0.0651]
Completeness to theta = 25.242°	99.2 %
Absorption correction	Semi-empirical from equivalents
Max. and min. transmission	1.000 and 0.828
Refinement method	Full-matrix least-squares on F^2
Data / restraints / parameters	6556 / 6 / 314
Goodness-of-fit on F^2	1.035
Final R indices [I>2sigma(I)]	R1 = 0.0709, wR2 = 0.1824
R indices (all data)	R1 = 0.1103, wR2 = 0.2076
Extinction coefficient	n/a
Largest diff. peak and hole	0.417 and -0.360 e.$Å^{-3}$

Table S2. Selected bond lengths (Å) and angles (^{o}) for spiro compound **I**.

C(1)-C(2)	1.378(3)
C(1)-O(1)	1.383(3)
C(1)-C(6)	1.402(3)
C(2)-C(3)	1.394(3)
C(2)-C(15)	1.511(3)
C(3)-C(4)	1.397(3)
C(4)-C(5)	1.404(3)
C(4)-C(7)	1.545(3)
C(5)-C(6)	1.395(3)
C(6)-C(11)	1.543(3)
C(15)-C(16)	1.515(3)
C(15)-C(20)	1.614(3)
C(19)-O(2)	1.218(3)
C(19)-C(24)	1.504(3)
C(19)-C(20)	1.533(3)
C(20)-O(1)	1.446(3)
C(20)-C(21)	1.494(3)
C(21)-C(22)	1.341(3)
C(22)-C(23)	1.467(3)

C(23)-C(24)	1.351(3)
C(2)-C(1)-O(1)	113.16(19)
C(2)-C(1)-C(6)	123.0(2)
O(1)-C(1)-C(6)	123.8(2)
C(1)-C(2)-C(3)	120.7(2)
C(1)-C(2)-C(15)	110.13(19)
C(3)-C(2)-C(15)	129.1(2)
C(2)-C(3)-C(4)	119.2(2)
C(3)-C(4)-C(5)	117.8(2)
C(3)-C(4)-C(7)	121.4(2)
C(5)-C(4)-C(7)	120.8(2)
C(6)-C(5)-C(4)	124.8(2)
C(5)-C(6)-C(1)	114.4(2)
C(5)-C(6)-C(11)	123.2(2)
C(1)-C(6)-C(11)	122.4(2)
C(6)-C(11)-C(12)	109.44(19)
C(10B)-C(7)-C(4)	112.2(4)
C(8A)-C(7)-C(4)	110.0(3)
C(10A)-C(7)-C(4)	108.1(2)
C(9A)-C(7)-C(4)	112.6(2)
C(4)-C(7)-C(9B)	108.7(4)
C(4)-C(7)-C(8B)	112.2(4)
C(9B)-C(7)-C(8B)	102.3(5)
C(2)-C(15)-C(16)	114.63(18)
C(2)-C(15)-C(20)	99.46(17)
C(16)-C(15)-C(20)	113.75(17)
O(2)-C(19)-C(24)	123.7(2)
O(2)-C(19)-C(20)	120.8(2)
C(24)-C(19)-C(20)	115.50(19)
O(1)-C(20)-C(21)	109.27(18)
O(1)-C(20)-C(19)	109.84(18)
C(21)-C(20)-C(19)	112.66(19)
O(1)-C(20)-C(15)	106.06(17)
C(21)-C(20)-C(15)	113.81(18)
C(19)-C(20)-C(15)	104.92(18)
C(22)-C(21)-C(20)	120.7(2)
C(21)-C(22)-C(23)	118.9(2)

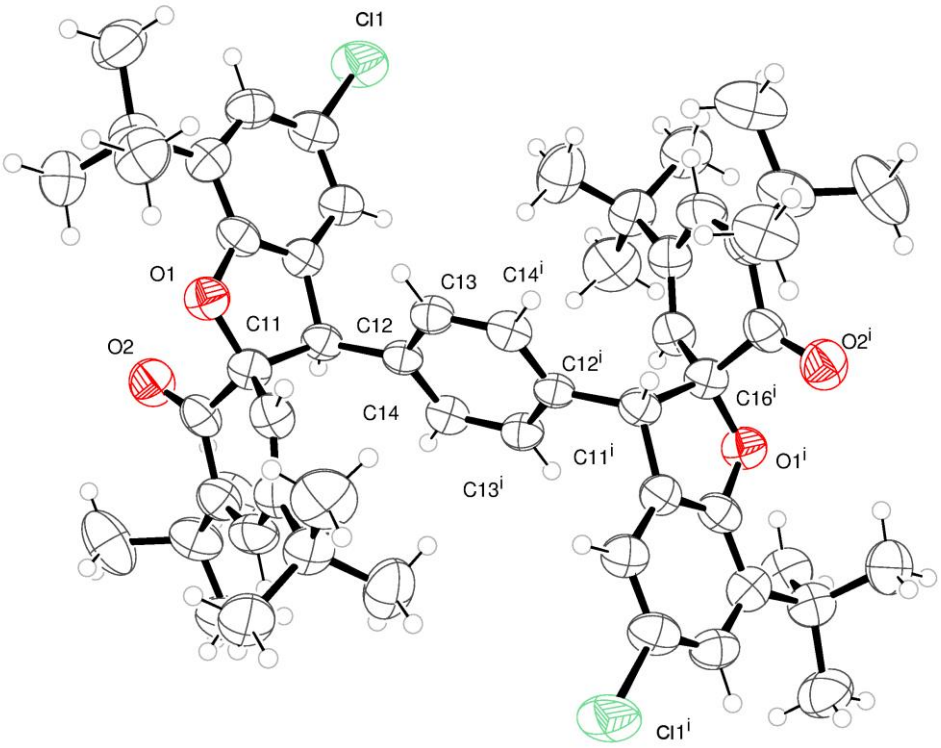

Figure S9. ORTEP diagram of spiro compound **II** with ellipsoids at 50 % probability level.

Table S3. Crystal data for spiro compound **II**.

Empirical formula	$C_{60}\ H_{74}\ Cl_2\ N_2\ O_4$	
Formula weight	958.11	
Temperature	150(2) K	
Wavelength	0.71073 Å	
Crystal system	Monoclinic	
Space group	P 2_1/n	
Unit cell dimensions	a = 14.9485(18) Å	α= 90°.
	b = 10.6228(7) Å	β= 112.770(9)°.
	c = 18.732(2) Å	γ = 90°.
Volume	2742.7(5) $Å^3$	
Z	2	
Density (calculated)	1.160 Mg/m^3	
Absorption coefficient	0.165 mm^{-1}	
F(000)	1028	
Crystal size	0.300 x 0.300 x 0.080 mm^3	
Theta range for data collection	1.491 to 25.625°.	

Index ranges	-18<=h<=12, -11<=k<=12, -22<=l<=22
Reflections collected	13127
Independent reflections	5146 [R(int) = 0.1061]
Completeness to theta = 25.000°	99.5 %
Absorption correction	Semi-empirical from equivalents
Max. and min. transmission	1.00 and 0.913
Refinement method	Full-matrix least-squares on F^2
Data / restraints / parameters	5146 / 0 / 317
Goodness-of-fit on F^2	0.825
Final R indices [I>2sigma(I)]	R1 = 0.0805, wR2 = 0.2044
R indices (all data)	R1 = 0.1552, wR2 = 0.2375
Extinction coefficient	n/a
Largest diff. peak and hole	0.258 and -0.678 e.$Å^{-3}$

Table S4: Selected bond lengths (Å) and angles (^{o}) for spiro compound **II**.

C(1)-O(1)	1.375(5)
C(1)-C(2)	1.379(6)
C(1)-C(6)	1.397(6)
C(2)-C(3)	1.399(6)
C(2)-C(11)	1.501(5)
C(3)-C(4)	1.377(6)
C(4)-C(5)	1.372(6)
C(4)-Cl(1)	1.765(4)
C(5)-C(6)	1.407(6)
C(6)-C(7)	1.518(6)
C(7)-C(9)	1.523(6)
C(7)-C(10)	1.524(7)
C(7)-C(8)	1.545(6)
C(11)-C(12)	1.527(5)
C(11)-C(16)	1.592(5)
C(12)-C(13)	1.374(5)
C(12)-C(14)	1.385(5)
C(13)-C(14)#1	1.399(5)
C(14)-C(13)#1	1.399(5)
C(15)-O(2)	1.240(4)
C(15)-C(20)	1.488(6)

C(15)-C(16)	1.518(6)
C(16)-O(1)	1.448(5)

O(1)-C(1)-C(2)	112.3(3)
O(1)-C(1)-C(6)	123.8(4)
C(2)-C(1)-C(6)	123.9(4)
C(1)-C(2)-C(3)	120.8(4)
C(1)-C(2)-C(11)	111.1(3)
C(3)-C(2)-C(11)	128.0(4)
C(4)-C(3)-C(2)	116.2(4)
C(5)-C(4)-C(3)	122.7(4)
C(5)-C(4)-Cl(1)	118.7(3)
C(3)-C(4)-Cl(1)	118.6(4)
C(4)-C(5)-C(6)	122.6(4)
C(1)-C(6)-C(5)	113.8(4)
C(1)-C(6)-C(7)	122.7(4)
C(5)-C(6)-C(7)	123.5(4)
C(6)-C(7)-C(9)	110.3(3)
C(6)-C(7)-C(10)	109.9(4)
C(9)-C(7)-C(10)	110.0(4)
C(6)-C(7)-C(8)	110.9(4)
C(9)-C(7)-C(8)	106.9(4)
C(10)-C(7)-C(8)	108.8(4)
C(2)-C(11)-C(12)	114.3(3)
C(2)-C(11)-C(16)	99.9(3)
C(12)-C(11)-C(16)	115.5(3)
C(13)-C(12)-C(14)	118.9(3)
C(13)-C(12)-C(11)	121.1(3)
C(14)-C(12)-C(11)	120.0(3)
C(12)-C(13)-C(14)#1	120.3(3)
C(12)-C(14)-C(13)#1	120.8(4)
O(2)-C(15)-C(20)	123.3(4)
O(2)-C(15)-C(16)	119.3(4)
O(1)-C(16)-C(17)	108.8(3)
O(1)-C(16)-C(15)	109.9(3)
O(1)-C(16)-C(11)	107.0(3)
C(17)-C(16)-C(11)	113.8(3)
C(1)-O(1)-C(16)	108.8(3)

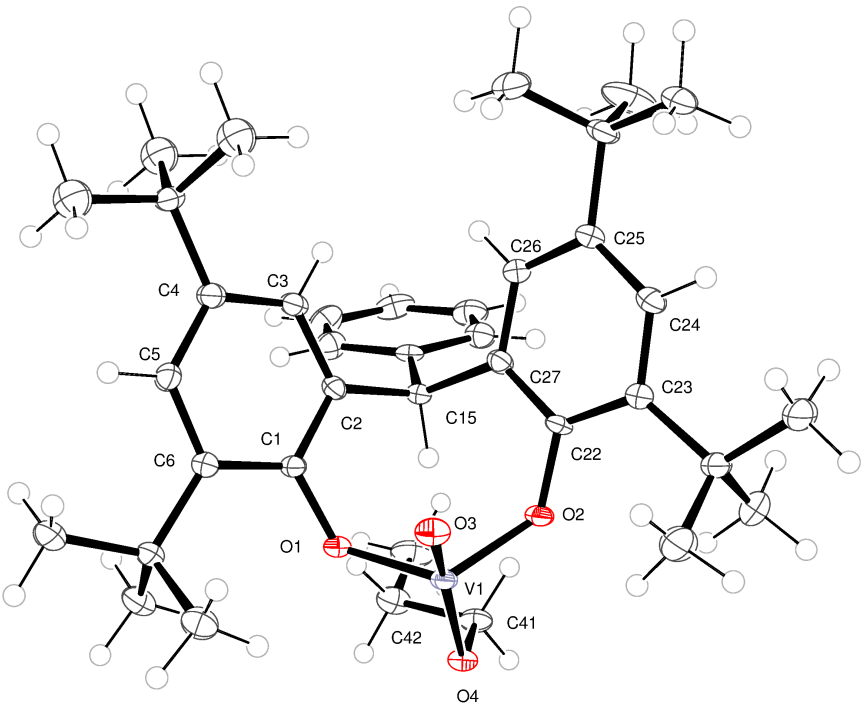

Figure S10. ORTEP diagram of complex **8** with ellipsoids at 50 % probability level.

Table S5. ^{51}V NMR data for compounds **1** – **8** (recorded in $CDCl_3$ at 298 K *versus* $VOCl_3$ as standard)

Compound	δ (ppm)	$\omega_{½}$ (Hz)
1	-433.3	170
2	-467.9	528
3	-432.5	170
4	-468.2, -558.5	277, 297
5	-467.7, -539.6	520, 296
6	-7.3	3373
7	-211.1	647
8	-433.6	170

Catalysis

Ethylene polymerization: results for the effect of co-catalyst and ETA

Table S6. Results for the effect of co-catalyst and ETA on compounds **1** - **3**, **5**, **8** and **[VO(OEt)Cl_2]**.[a]

Run	Pre-Cat	Co-Cat	Al/V	ETA/V	T[c]	Yield[b]	Activity[d]	M_w	M_n	PDI
1	**1**	DMAC	5000		30	0.068	6,800			
2			20000		30	0.128	12,800	2,261,718	547,734	4.1
3			5000	5000	30	0.454	45,400			
4			20000	20000	30	0.534	53,400	974,413	116,671	8.4
5		DEAC	5000		30	0.022	2,200			
6			20000		30	0.009	900	455,970	88,930	5.1
7			5000	5000	30	0.36	36,000			
8			20000	20000	10[e]	0.811	243,400	73,074	25,671	2.9
9		EADC	5000		30	0.034	3,400			
10			20000		30	0.05	5,000	228,678	94,326	2.4
11			5000	5000	30	0.304	30,400			
12			20000	20000	30	0.338	33,800	749,498	205,539	3.7
13		EASC	5000		30	0.061	6,100			
14			20000		30	0.058	5,800	943,144	353,483	2.7
15			5000	5000	30	0.292	29,200			
16			20000	20000	30	0.358	35,800	666,983	160,727	4.2
17	**2**	DMAC	20000	20000	30	0.306	122,200	1,180,000	241,000	4.9
18		DEAC	20000	20000	30	0.231	92,300	1,040,000	103,000	10.0
19	**3**	DMAC	5000		30	0.14	14,000			
20			20000		30	0.112	11,200	3,290,580	1,349,253	2.44
21			5000	5000	30	0.388	38,800			
22			20000	20000	30	0.45	45,000	865,647	81,817	10.6
23		DEAC	5000		30	0.011	1,100			
24			20000		30	0.015	1,500			
25			5000	5000	30	0.323	32,300			
26			20000	20000	30	0.494	49,400	267,660	45,443	5.9
27		EADC	5000		30	0.014	1,400			
28			20000		30	0.01	1000	196,554	57,342	3.4
29			5000	5000	30	0.31	31,000			
30			20000	20000	30	0.472	47,200	749,897	70,411	10.6
31		EASC	5000		30	0.038	3,800			
32			20000		30	0.034	3,400	967,997	315,747	3.1
33			5000	5000	30	0.297	29,700			
34			20000	20000	30	0.438	43,800	273,709	27,818	9.8
35	**5**	DMAC	20000	20000	30	0.256	102,200	814,000	123,000	6.6
36		DEAC	20000	20000	30	0.237	94,700	933,000	88,800	10.5
37	**8**	DMAC	5000		30	0.192	19,200			
38			20000		30	0.341	34,100	1,683,732	57,625	29.2
39			5000	5000	30	0.343	34,300			
40			20000	20000	30	0.423	42,300	1,067,563	120,753	8.84
41		DEAC	5000		30	0.084	8,400			

42			20000		30	0.039	3,900	333,763	104,963	3.2
43			5000	5000	30	0.303	30,300			
44			20000	20000	15[e]	0.527	105,400	110,765	26,097	4.2
45		EADC	5000		30	0.0198	2,000			
46			20000		30	0.0107	1,100	181,151	68,551	2.6
47			5000	5000	30	0.3232	32,300			
48			20000	20000	23[e]	0.538	70,200	547,756	135,546	4.0
49		EASC	5000		30	0.0319	3,200			
50			20000		30	0.0305	3,100	874,365	191,854	4.6
51			5000	5000	30	0.2947	29,500			
52			20000	20000	22[e]	0.4951	67,500	216,581	29,627	7.3
53	**[VO(OEt)Cl_2]**	DMAC	5000		30	0.16	32,000			
54			20000		30	0.106	21,200	2,114,696	740,175	2.9
55			5000	5000	30	0.368	73,600			
56			20000	20000	30	0.429	85,800	1,787,338	385,401	4.6
57		DEAC	5000		30	0.009	1,700			
58			20000		30	0.001	100			
59			5000	5000	30	0.257	51,400			
60			20000	20000	30	0.343	68,600	139,330	48,676	2.9
61		EADC	5000		30	0.011	1,100			
62			20000		30	0.001	100			
63			5000	5000	30	0.272	27,200			
64			20000	20000	30	0.375	37,500	711,232	187,694	3.8
65		EASC	5000		30	0.019	1,900			
66			20000		30	0.014	1,400			
67			5000	5000	30	0.317	31,700			
68			20000	20000	30	0.341	34,100	387,638	99,975	3.9

[a] **Conditions**: 50 °C, 5 mL toluene, 0.01 µmol V, 0.8 MPa ethylene, reaction quenched with isobutyl alcohol; [b] grams, [c] minutes, [d](g/(mmol.hr)), [e] polymerization was stopped due to consumption of stock ethylene.

Figure S11: Ethylene uptake for **1** *versus* time using DMAC (left) and DEAC (right) as co-catalyst.

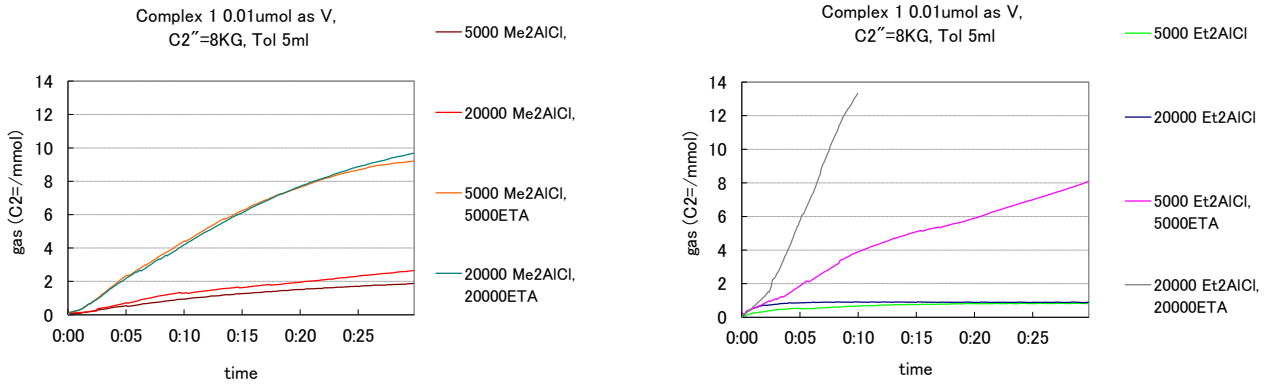

Figure S12: Ethylene uptake for **1** *versus* time using EADC (left) and $Et_3Al_2Cl_3$ (SQ) (right) as co-catalyst.

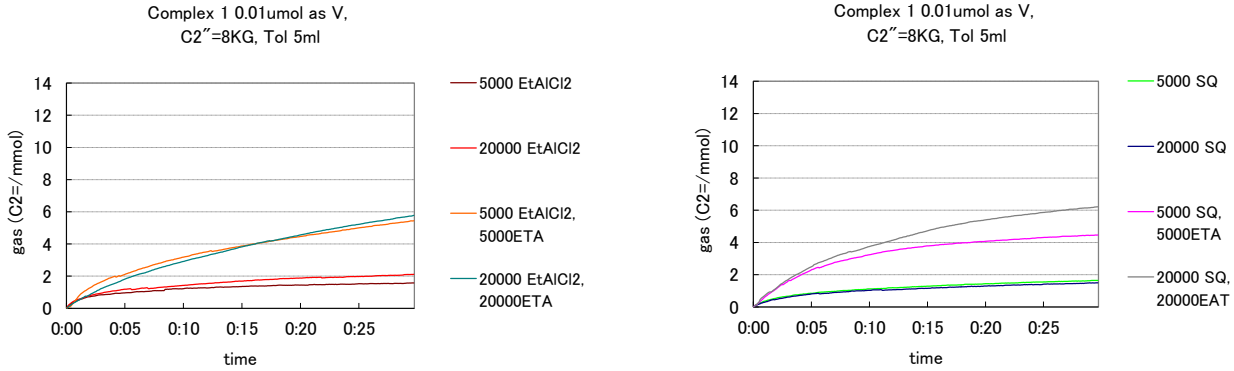

Figure S13: PDI graph for **1** using DMAC, DEAC, EADC and $Et_3Al_2Cl_3$ (SQ) as co-catalyst.

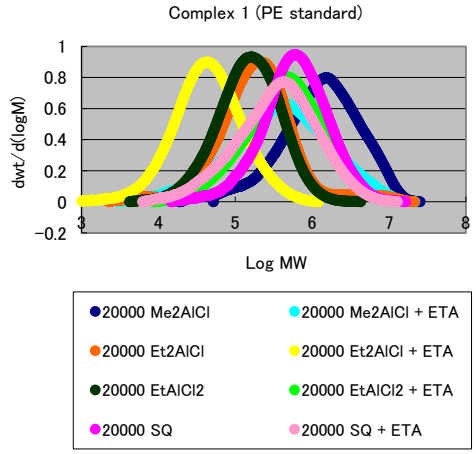

Figure S14: Ethylene uptake for **2** *versus* time using DMAC (left) and DEAC (right) as co-catalyst.

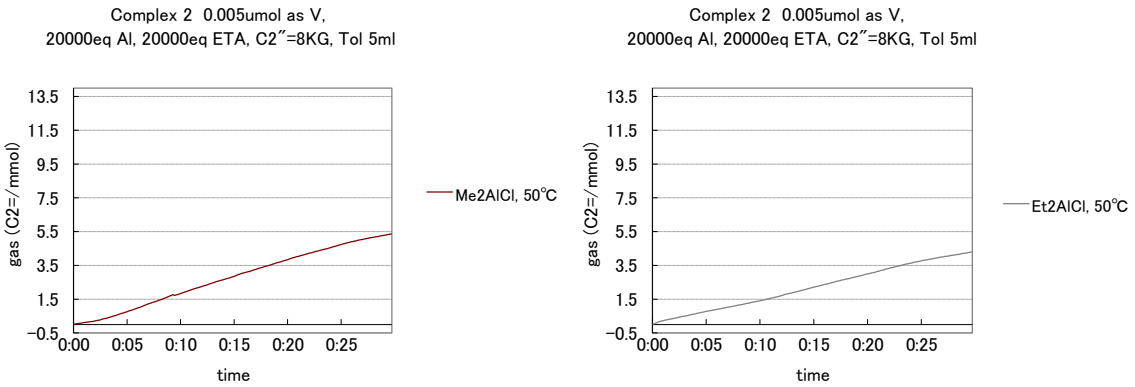

Figure S15: PDI graph for **2** using DMAC and DEAC as co-catalyst.

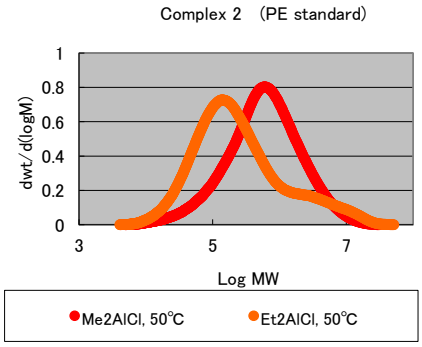

Figure S16: Ethylene uptake for **3** *versus* time using DMAC (left) and DEAC (right) as co-catalyst.

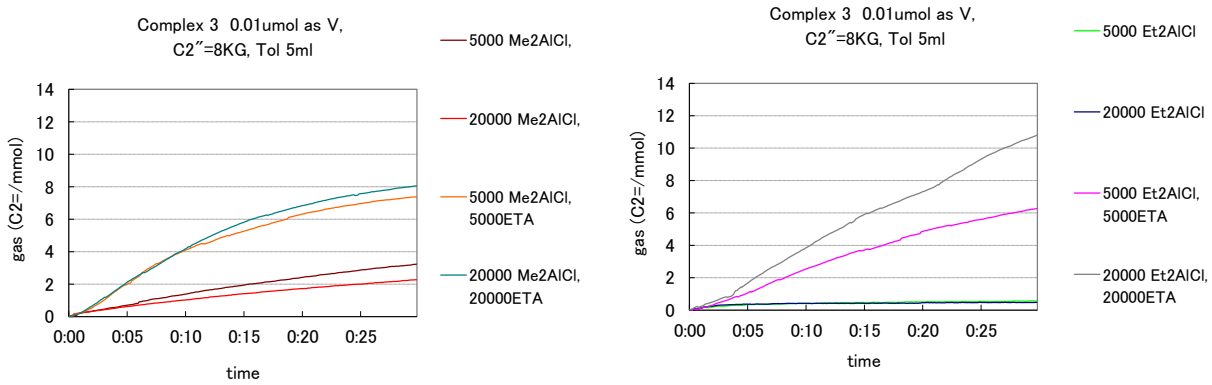

Figure S17: Ethylene uptake for **3** *versus* time using EADC (left) and Et_3AlCl_2 (SQ) (right) as co-catalyst.

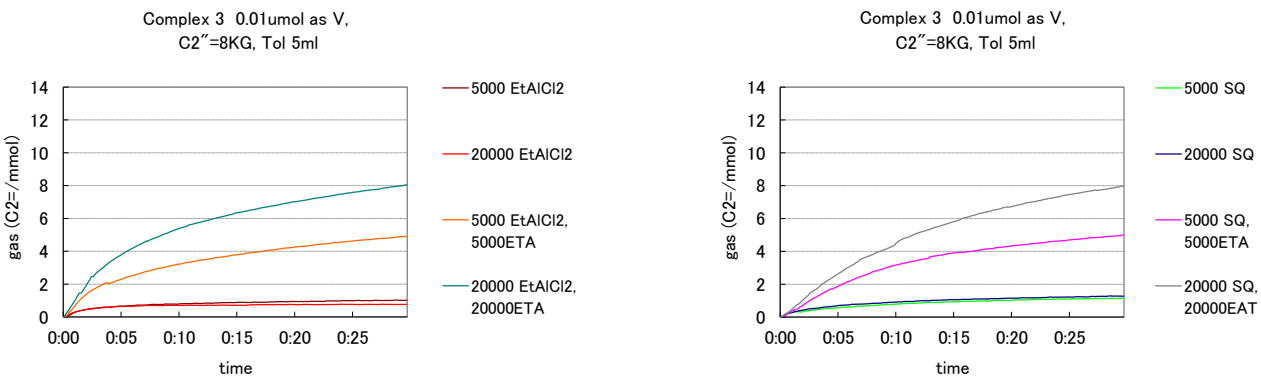

Figure S18: PDI graph for **3** using DMAC, DEAC, EADC and Et_3AlCl_2 (SQ) as co-catalyst.

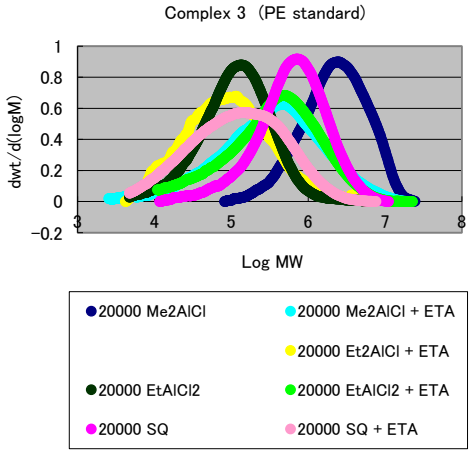

Figure S19: Ethylene uptake for **5** *versus* time using DMAC (left) and DEAC (right) as co-catalyst.

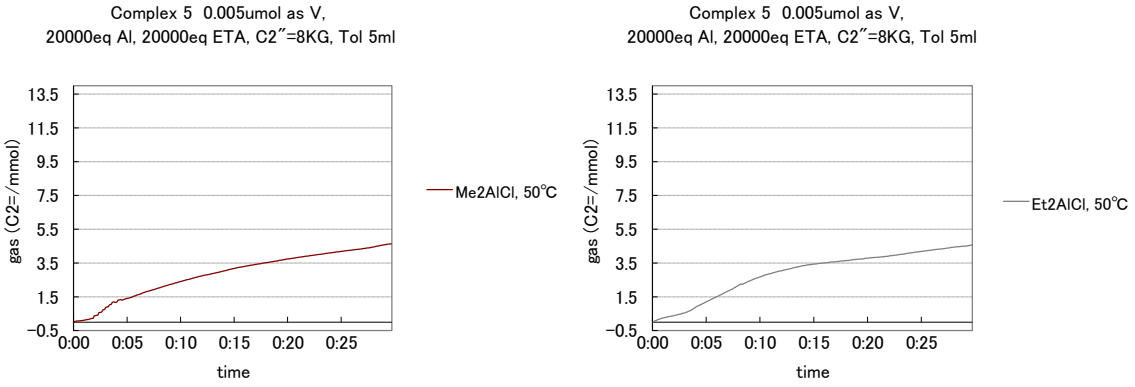

Figure S20: PDI graph for **5** using DMAC and DEAC as co-catalyst.

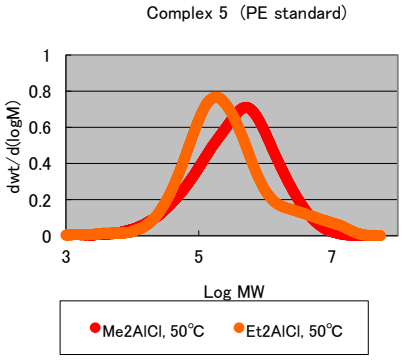

Figure S21: Ethylene uptake for **8** *versus* time using DMAC (left) and DEAC (right) as co-catalyst.

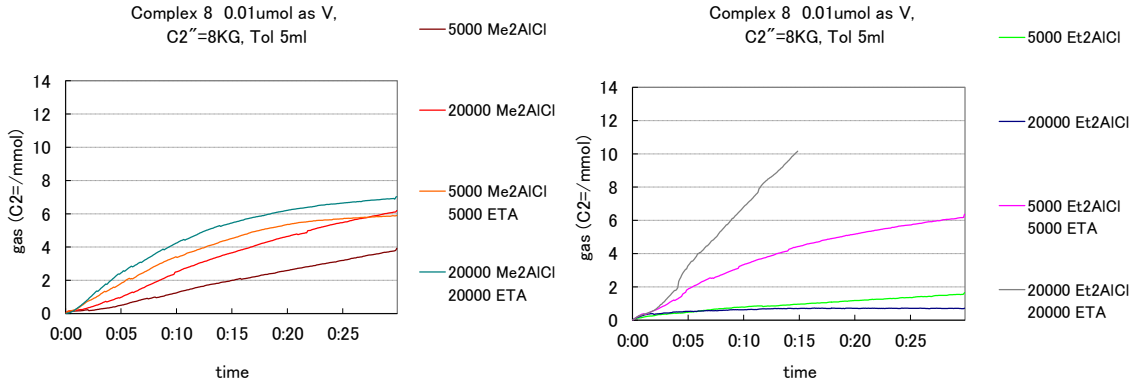

Figure S22: Ethylene uptake for **8** *versus* time using EADC (left) and Et_3AlCl_2 (SQ) (right) as co-catalyst.

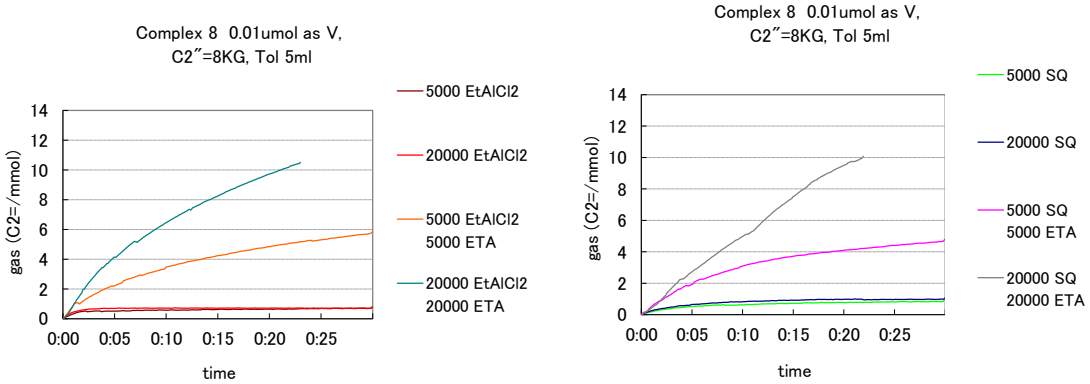

Figure S23: PDI graph for **8** using DMAC, DEAC, EADC and Et_3AlCl_2 (SQ) as co-catalyst.

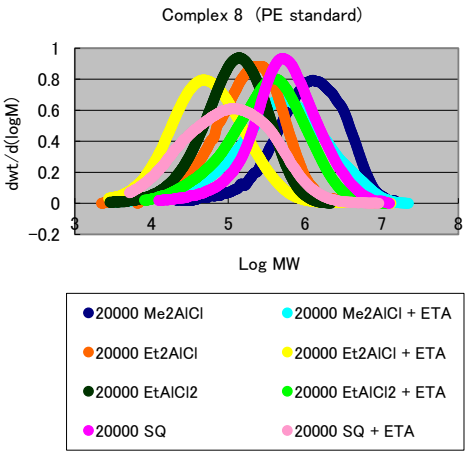

Figure S24: Ethylene uptake for $VO(OEt)Cl_2$ *versus* time using DMAC (left) and DEAC (right) as co-catalyst.

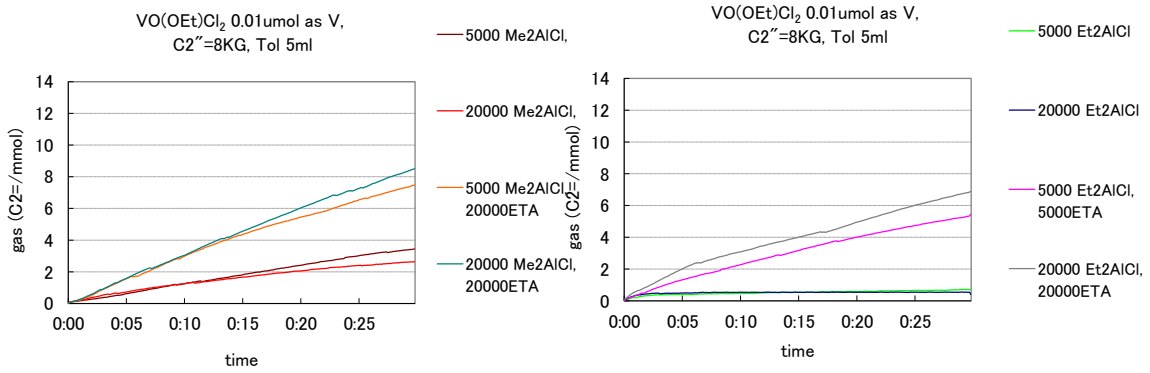

Figure S25: Ethylene uptake for $VO(OEt)Cl_2$ *versus* time using EADC (left) and Et_3AlCl_2 (SQ) (right) as co-catalyst.

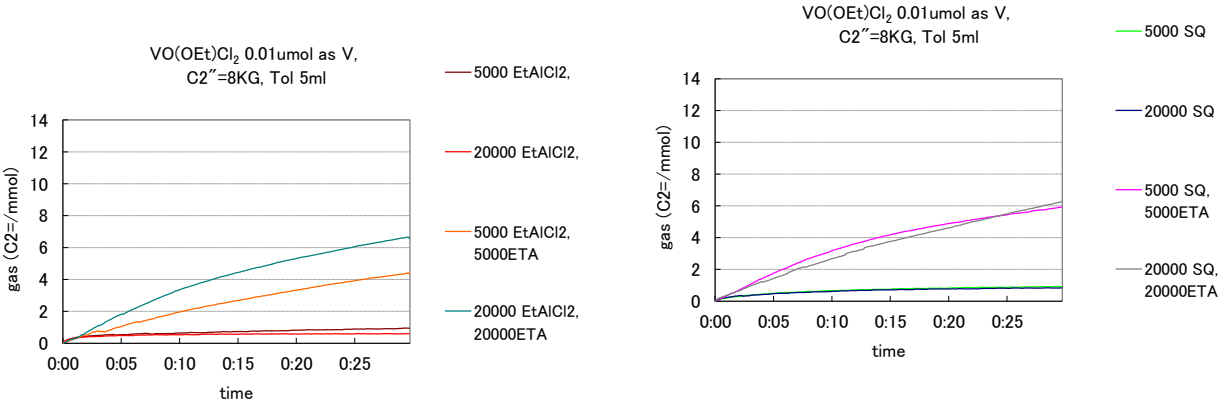

Figure S26: PDI graph for $VO(OEt)Cl_2$ using DMAC, DEAC, EADC and Et_3AlCl_2 (SQ) as co-catalyst.

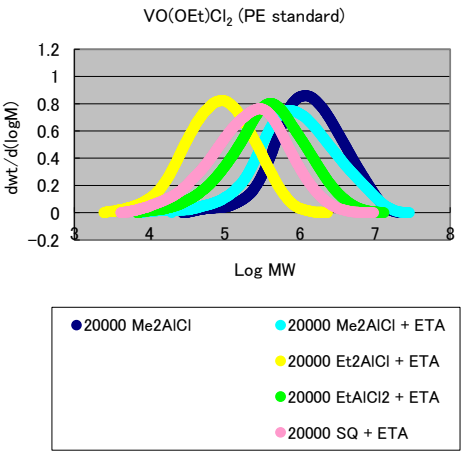

Ethylene polymerization: results for the effect of temperature

Table S7. Effect of temperature on compounds **1 - 3**, **5 - 8** and $[VO(OEt)Cl_2]$.[a]

Run	Pre-Cat	Co-Cat	Temp[c]	T[d]	Yield[b]	Activity[e]	M_w	M_n	PDI	T_m[c]
1	**1**	DMAC	50	30	0.422	168,800	467,300	67,300	6.9	137.2
2			80	30	0.41	163,900	136,100	44,500	3.1	133.2
3			110	30	0.081	32,600				134.8
4			140	30	-	-				
5		DEAC	50	30	0.283	113,200	254,000	38,900	6.5	135.4
6			80	30	0.355	14,8000	135,800	20,600	6.7	136.1
7			110	30	0.07	28,000				132.2
8			140	30	0.031	12,500				130.2
9	**2**	DMAC	50	30	0.306	122,200	1,180,000	241,000	4.9	136.1
10			80	30	0.217	86,800	249,000	26,800	9.3	136.0
11			110	30	0.087	34,800	65,300	21,400	3.1	134.6
12			140	30	0.024	9,700	-	-	-	132.2
13		DEAC	50	30	0.231	92,300	1,040,000	103,000	10.0	131.8
14			80	30	0.110	44,100	82,000	18,800	4.4	134.3
15			110	30	0.039	15,500	18,900	9,200	2.1	133.1
16			140	30	0.015	6,000	-			131.0
17	**3**	DMAC	50	30	0.357	142,800	536,200	93,900	5.7	132.0
18			80	30	0.301	120,600	173,800	60,400	2.9	133.0
19			110	30	0.062	24,700				135.0
20			140	30	-	-				
21		DEAC	50	30	0.218	87,400	555,100	84,000	6.6	134.0
22			80	30	0.046	18,400	366,500	34,900	10.5	133.0
23			110	30	-	-				
24			140	30	-	-				
25	**5**	DMAC	50	30	0.256	102,200	814,000	123,000	6.6	131.9
26			80	30	0.224	89,700	163,000	44,800	3.6	133.5
27			110	30	0.044	17,600	-	-	-	133.0
28			140	30	0.000	0	-	-	-	-
29		DEAC	50	30	0.237	94,700	933,000	88,800	10.5	132.2
30			80	30	0.040	16,200	142,000	16,100	8.8	133.1
31			110	30	0.029	11,600	-	-	-	133.3
32			140	30	0.006	2,500	-	-	-	131.4
33	**6**	DMAC	50	30	0.3099	124,000	1,430,000	265,000	5.4	136.8
34			80	30	0.034	13,600	119,000	30,800	3.8	134.3
35			110	30	0	0				
36			140	30	0	0				
37		DEAC	50	30	0.5899	236,000	162,000	62,800	2.6	135.1
38			80	30	0.1439	57,600	65,800	35,000	1.9	134.1
39			110	30	0	0				
40			140	30	0	0				

41	**7**	DMAC	50	30	119.84	119,800	996,000	132,000	7.5	134.3
42			80	30	32.56	32,600	131,000	52,800	2.5	133.7
43			110	30	0	0				
44			140	30	0	0				
45		DEAC	50	30	0.4856	194,200	173,000	58,600	3.0	134.6
46			80	30	0.0709	28,400	72,400	39,500	1.8	133.6
47			110	30	0	0				
48			140	30	0	0				
49	**8**	DMAC	50	30	0.311	124,400	783,800	115,000	6.8	
50			80	30	0.402	161,000	188,000	67,800	2.8	
51			110	30	0.065	25,900				
52			140	30	0.002	900				
53		DEAC	50	30	0.215	86,100	671,700	88,100	7.6	
54			80	30	0.056	22,600	313,500	35,800	8.8	
55			110	30	0.02	8,200				
56			140	30	0.005	1,800				
57	**[VO(OEt)Cl_2]**	DMAC	50	30	0.374	74,700	945,800	168,700	5.6	134.7
58			80	30	0.354	70,800	137,600	45,700	3.0	133.3
59			110	30	0.097	19,400				134.5
60			140	30	-	-				
61		DEAC	50	30	0.483	96,700	316,500	56,800	5.6	134.4
62			80	30	0.237	47,400	208,700	27,200	7.7	134.0
63			110	30	0.087	17,300				133.8
64			140	30	0.018	3,600				128.9

[a] **Conditions**: 5 mL toluene, 0.005 µmol V, 0.8 MPa ethylene, 20,000 equivalents Co-catalyst, 20,000 equivalents ETA, reaction quenched with *iso*-butyl alcohol; [b] grams, [c] °C, [d] minutes, [e] (g/(mmol.hr)).

Figure S27: Ethylene uptake for **1** *versus* time using DMAC (left) and DEAC (right) as co-catalyst.

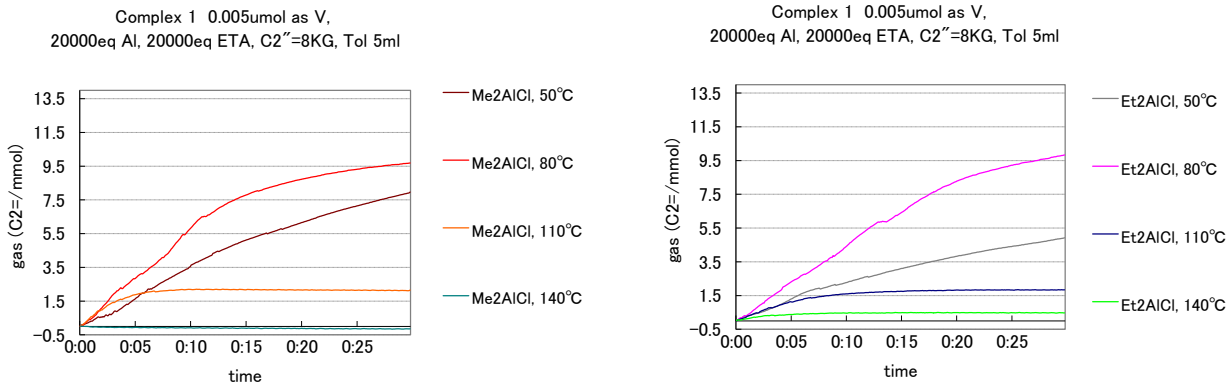

Figure S28: PDI graph for **1** using DMAC and DEAC as co-catalyst.

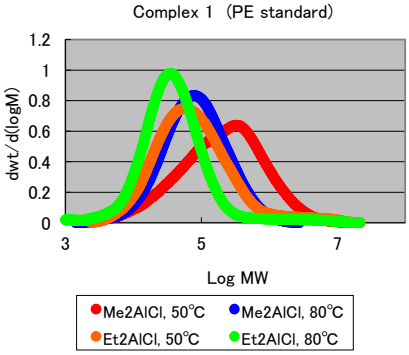

Figure S29: Ethylene uptake for **2** *versus* time using DMAC (left) and DEAC (right) as co-catalyst.

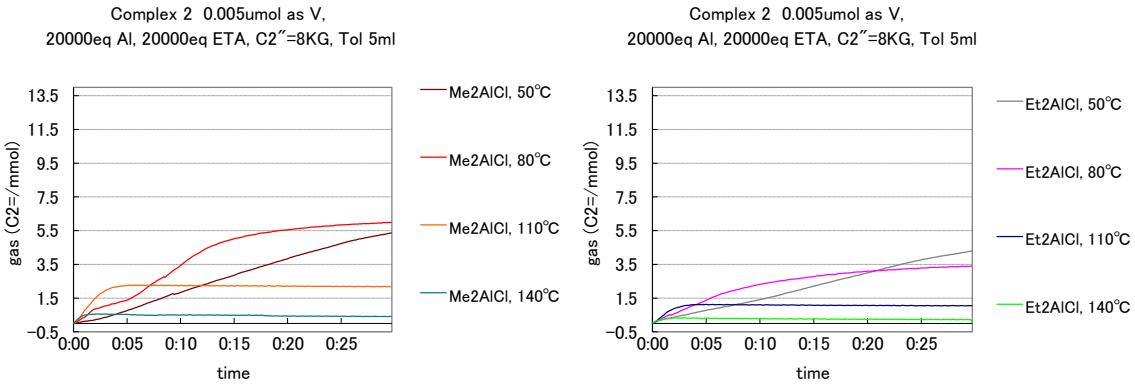

Figure S30: PDI graph for **2** using DMAC and DEAC as co-catalyst.

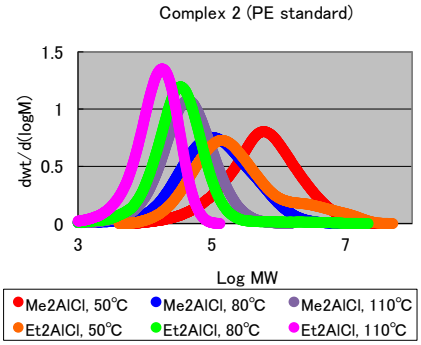

Figure S31: Ethylene uptake for **3** *versus* time using DMAC (left) and DEAC (right) as co-catalyst.

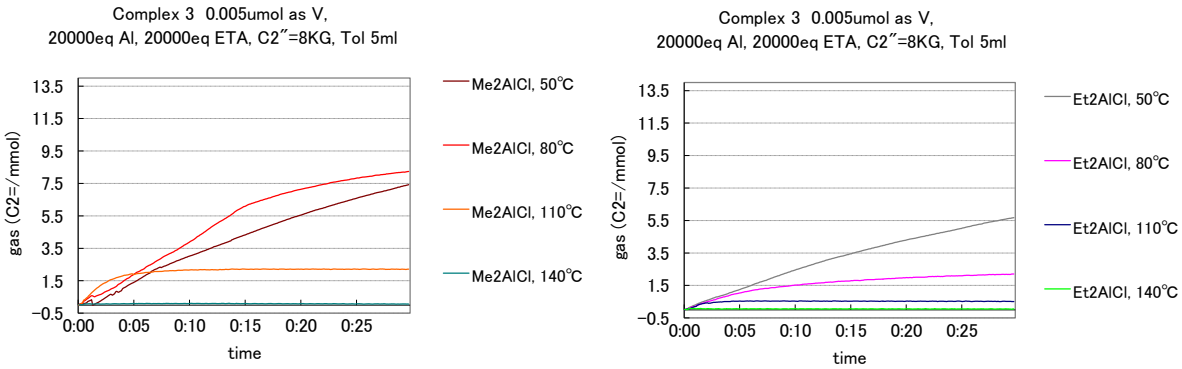

Figure S32: PDI graph for **3** using DMAC and DEAC as co-catalyst.

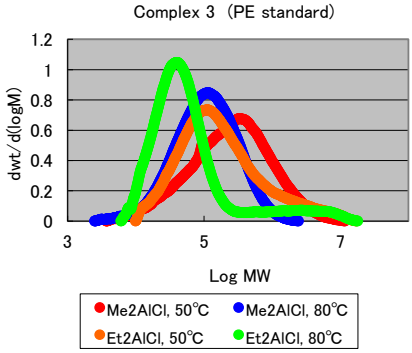

Figure S33: Ethylene uptake for **5** *versus* time using DMAC (left) and DEAC (right) as co-catalyst.

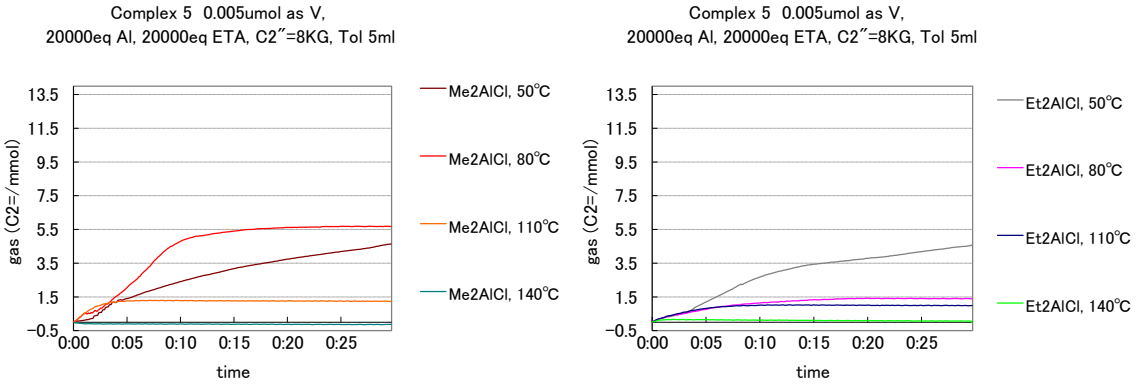

Figure S34: PDI graph for **5** using DMAC and DEAC as co-catalyst.

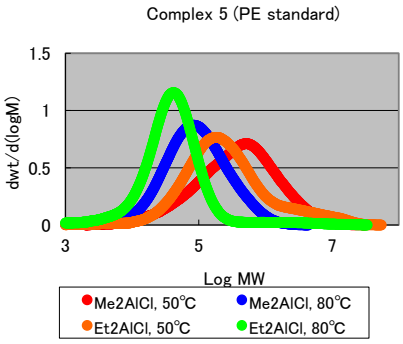

Figure S35: Ethylene uptake for **6** *versus* time using DMAC (left) and DEAC (right) as co-catalyst.

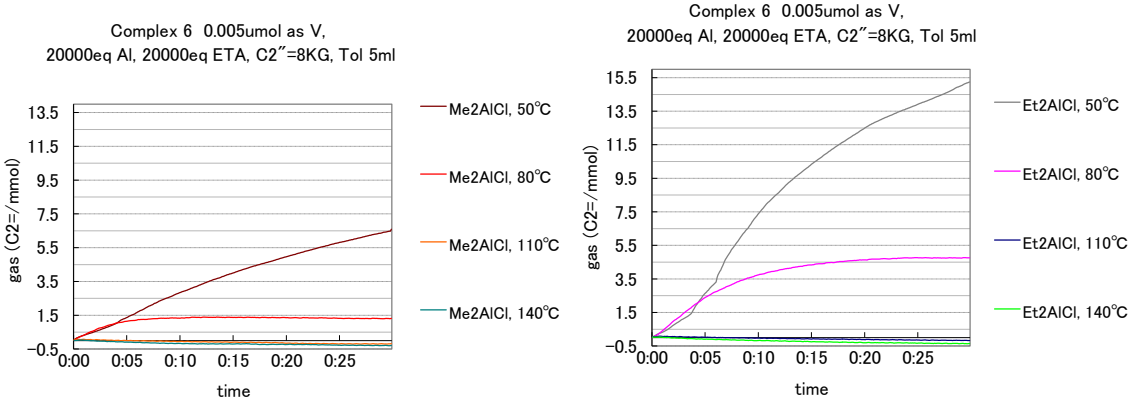

Figure S36: PDI graph for **6** using DMAC and DEAC as co-catalyst.

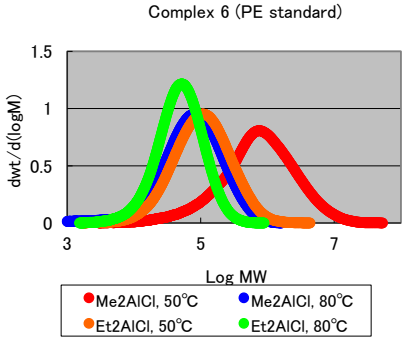

Figure S37: Ethylene uptake for **7** *versus* time using DMAC (left) and DEAC (right) as co-catalyst.

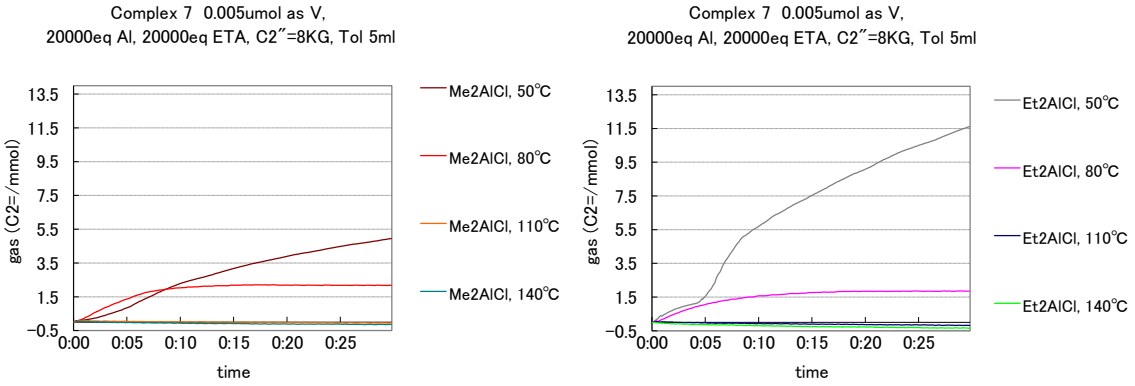

Figure S38: PDI graph for **7** using DMAC and DEAC as co-catalyst.

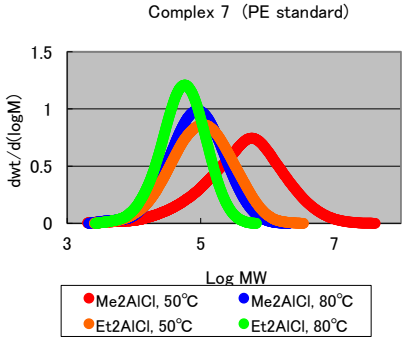

Figure S39: Ethylene uptake for **8** *versus* time using DMAC (left) and DEAC (right) as co-catalyst.

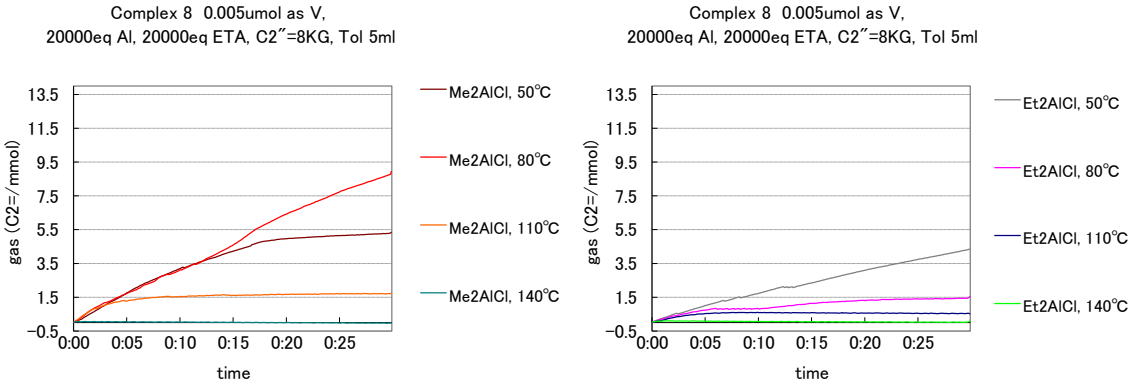

Figure S40: PDI graph for **8** using DMAC and DEAC as co-catalyst.

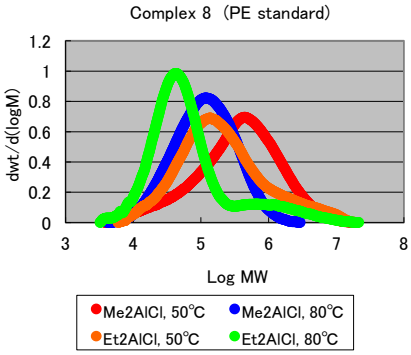

Figure S41: Ethylene uptake for $VO(OEt)Cl_2$ *versus* time using DMAC (left) and DEAC (right) as co-catalyst.

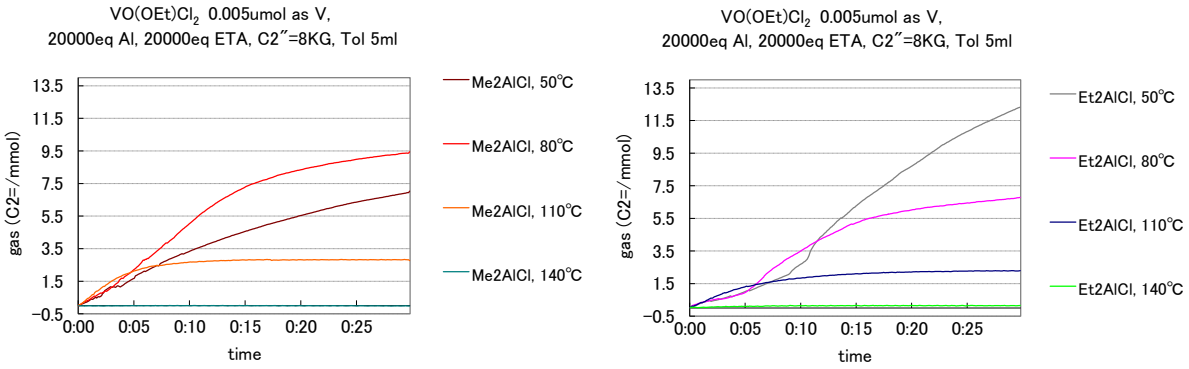

Figure S42: PDI graph for $VO(OEt)Cl_2$ using DMAC and DEAC as co-catalyst.

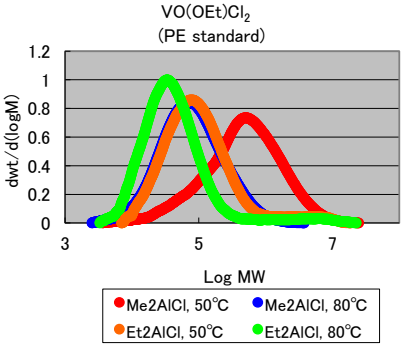

Figure S43. ^{13}C NMR spectrum of polyethylene using complex **2**/Et_3AlCl_2 (run 31, Table S6).

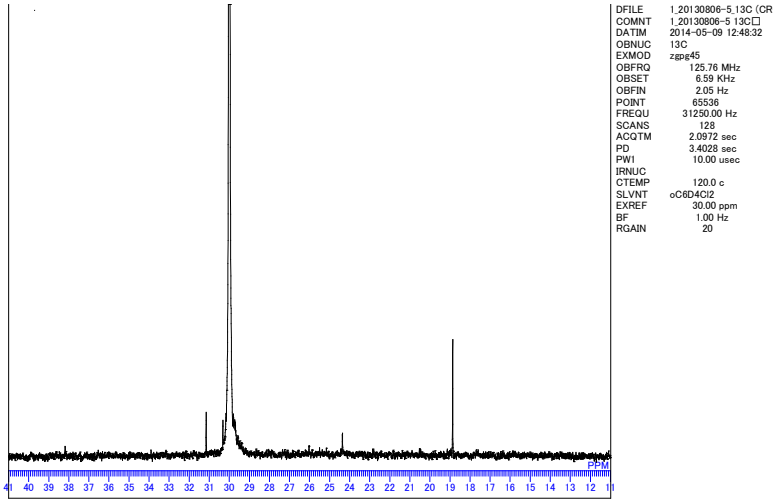

Table S8. Data for runs using **1** and **3** with co-catalysts Me_3Al, Et_3Al and DMAO.

		Complex 1	Complex 1	Complex 1	Complex 1	Complex 3	Complex 3	Complex 3	Complex 3
As Cat	(μmol)	0.005	0.005	0.005	0.005	0.005	0.005	0.005	0.005
As Vanadium	(μmol)	0.01	0.01	0.01	0.01	0.01	0.01	0.01	0.01
ETA	(M)		0.10	0.10	0.10		0.10	0.10	0.10
ETA/V	(eq)		20000	20000	20000		20000	20000	20000
	(mmol)		0.20	0.20	0.20		0.20	0.20	0.20
Co-catalyst		**Me3Al**	**Me3Al**	**Et3Al**	**DMAO**	**Me3Al**	**Me3Al**	**Et3Al**	**DMAO**
Al/V	(eq)	20000	20000	20000	20000	20000	20000	20000	20000
	(mmol)	0.2000	0.2000	0.2000	0.2000	0.2000	0.2000	0.2000	0.2000
Ethylene	(MPa)	0.8	0.8	0.8	0.8	0.8	0.8	0.8	0.8
Toluene (total)	(ml)	5.0	5.0	5.0	5.0	5.0	5.0	5.0	5.0
Temp	(℃)	50	50	50	50	50	50	50	50
Time	(min)	**30**	**30**	**30**	**30**	**30**	**30**	**30**	**30**
Yield	(g)	0.000	0.000	0.000	0.000	0.000	0.000	0.000	0.000
Activity by weight (kg/mmol V・h)		–	–	–	–	–	–	–	–
Activity by C2 uptake at 20min		–	–	–	–	–	–	–	–
Activity by C2 uptake at 5min		–	–	–	–	–	–	–	–
Ratio (20min/5min)		–	–	–	–	–	–	–	–

Table S9. Data for runs using **8** and $VO(OEt)Cl_2$ with Me_3Al, Et_3Al and DMAO.

		Complex 8	Complex 8	Complex 8	Complex 8	VO(OEt)Cl2	VO(OEt)Cl2	VO(OEt)Cl2	VO(OEt)Cl2
As Cat	(μmol)	0.005	0.005	0.005	0.005	0.005	0.005	0.005	0.005
As Vanadium	(μmol)	0.01	0.01	0.01	0.01	0.01	0.01	0.01	0.01
ETA	(M)		0.10	0.10	0.10		0.10	0.10	0.10
ETA/V	(eq)		20000	20000	20000		20000	20000	20000
	(mmol)		0.20	0.20	0.20		0.20	0.20	0.20
Co-catalyst		**Me3Al**	**Me3Al**	**Et3Al**	**DMAO**	**Me3Al**	**Me3Al**	**Et3Al**	**DMAO**
Al/V	(eq)	20000	20000	20000	20000	20000	20000	20000	20000
	(mmol)	0.2000	0.2000	0.2000	0.2000	0.2000	0.2000	0.2000	0.2000
Ethylene	(MPa)	0.8	0.8	0.8	0.8	0.8	0.8	0.8	0.8
Toluene (total)	(ml)	5.0	5.0	5.0	5.0	5.0	5.0	5.0	5.0
Temp	(℃)	50	50	50	50	50	50	50	50
Time	(min)	**30**	**30**	**30**	**30**	**30**	**30**	**30**	**30**
Yield	(g)	0.000	0.000	0.000	0.000	0.000	0.000	0.000	0.000
Activity by weight (kg/mmol V・h)		–	–	–	–	–	–	–	–
Activity by C2 uptake at 20min		–	–	–	–	–	–	–	–
Activity by C2 uptake at 5min		–	–	–	–	–	–	–	–
Ratio (20min/5min)		–	–	–	–	–	–	–	–

Ethylene/propylene co-polymerization

Figure S44: Ethylene uptake for **1 - 3**, **5 - 8** and $VO(OEt)Cl_2$ *versus* time using DMAC (left) and using DEAC (right) as co-catalyst.

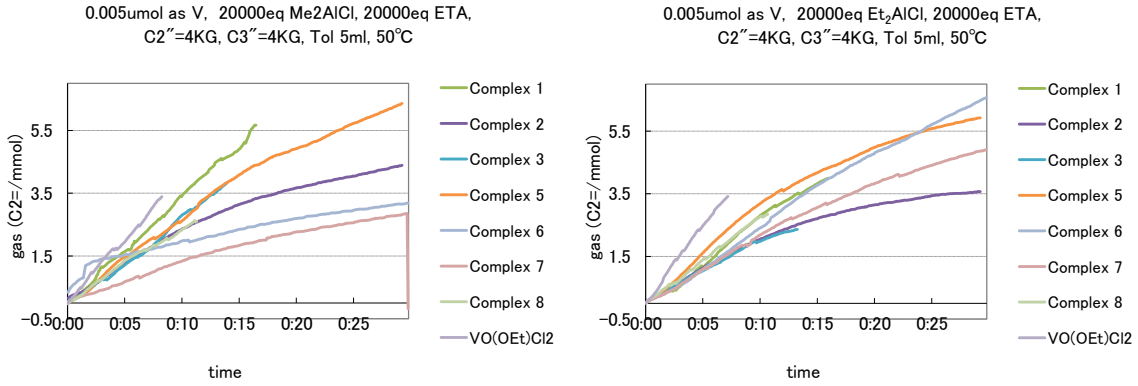

Note: Co-polymerization was continued for 30 min for all the catalysts, but the ethylene uptake data for **1**, **3** and **8** were lost from the middle of the experiment due to mechanical trouble.

Figure S45: PDI graph for **1 -3**, **5 - 8** and $VO(OEt)Cl_2$ using DMAC as co-catalyst.

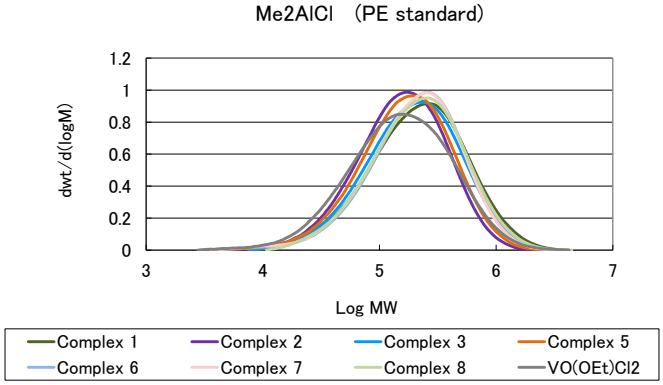
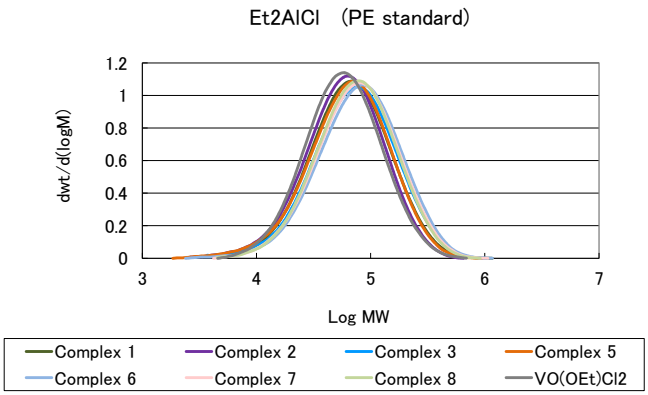
Figure S46: PDI graph for **1 - 3**, **5 - 8** and $VO(OEt)Cl_2$ using DEAC as co-catalyst.